

# INTERACTIONS IN NATURAL CONVECTION FROM AN ARRAY OF HEATED ELEMENTS, EXPERIMENTAL

J. LIEBERMAN

Eastman Kodak Company, Rochester, New York

B. GEBHART

Department of Thermal Engineering, Cornell University, Ithaca, New York

(Received 26 November 1968 and in revised form 14 March 1969)

**Abstract**—Interactions between the separate natural convection flows induced by individual surfaces in a close spaced array are studied for various arrangements of spacing and orientation. The effects on heat transfer and on the induced flow and temperature field are determined. The causes of various effects are inferred from interferograms of the near temperature field and the rising plume. Certain relations between effects are apparent and are explicable in direct physical terms, although no analysis is given. It is clear from these results that interaction effects may be profitably optimized for particular ends.

## NOMENCLATURE

$D$ , wire diameter;  
 $g$ , gravitational constant;  
 $h$ , local convection coefficient of wire;  
 $h_0$ , convection coefficient of lowest wire;  
 $\bar{h}$ , average convection coefficient of array;  
 $q''$ , wire heat flux;  
 $T_w$ , temperature of each wire;  
 $T_{w0}$ , temperature of lowest wire;  
 $T_\infty$ , ambient air temperature;  
 $\Delta T$ , temperature excess ( $T_w - T_\infty$ );  
 $X$ ,  
 $Y$ ,  
 $Z$  } spatial coordinates;  
 $X_L$ , width of the array;  
 $B$ , coefficient of expansion of air;  
 $k$ , thermal conductivity of air;  
 $\nu$ , kinematic viscosity of air;  
 $Gr_{XL}$ , Grashof number based on array width  
 $\left(\frac{gB\Delta T(X_L)^3}{\nu^2}\right)$ ;  
 $Gr_D$ , Grashof number based on wire diameter  
 $\left(\frac{gB\Delta T D^3}{\nu^2}\right)$ ;  
 $Gr_{q,D}$ , flux Grashof number based on wire diameter  
 $\left(\frac{gBq''D^4}{k\nu^2}\right)$ ;

$Nu$ , Nusselt number ( $hD/k$ );  
 $Nu_0$ , Nusselt number of lowest wire ( $h_0D/k$ );  
 $\bar{Nu}_m$ , average Nusselt number ( $\bar{h}D/k$ ).

## INTRODUCTION

THE PROBLEM studied in this paper is the effect in natural convection of orientation and spacing on the heat transfer rate and induced temperature distributions for a finite flat array of long horizontal wires.

Arrays of heating elements are found in many natural convection situations such as, for example, in the heating of heavy crude oil in storage to ease pumping requirements. It is possible that there may be an optimum spacing, grouping and orientation, for maximum heating efficiency for such configurations. Arrays of piping are used in processing plants to transport hot liquids from one location to another. Here the choice of the proper configuration might service to increase or to decrease heat losses.

There are also many applications where groups of small heating elements must be cooled. An example are the tubes, resistors, transistors, etc. in an electronic device. The proper grouping of elements could be useful for maximizing the cooling effects.

The ratio of the wire diameter to the spacing

between the wires in the array used for this investigation was too small to approximate the industrial applications that have been mentioned. However the results clearly delineate many features of such processes.

While there is no analytical or experimental information available concerning extensive arrays of elements, there have been heat-transfer investigations of several grouped tubes and of single cylinders that give some insight into the problem.

In 1948, Eckert and Soehngen [1] measured Nusselt numbers for multiple isothermal horizontal tubes of 0.878 in. dia. The Grashof number for a single tube at the test condition, based on tube diameter, was 34 300. It was found that for horizontal tubes located directly above each other, the Nusselt number, based on the average convection coefficient, decreased as additional tubes were added to the array. For two horizontal tubes the upper tube's Nusselt number was 87 per cent of the value for the lower tube, which had the same Nusselt number as a single tube. When a third tube was added, the Nusselt number of the lowest tube remained the same, that of the second tube decreased to 83 per cent of that of the lowest tube and the third tube's Nusselt number was only 65 per cent of that of the lowest tube.

The tubes were also arranged so that the axes of the highest and lowest tubes were in the same vertical plane, while the axis of the middle tube was offset by a half tube diameter. The lowest tube still had the same Nusselt number as a single horizontal tube, the middle tube's Nusselt number was 103 per cent of that of the lowest tube and the highest tube had a Nusselt number which was 86 per cent of the lowest tube's value. Thus, the staggered arrangement had a higher average Nusselt number than the configuration with the three tubes directly over each other.

In the explanation of these results, Eckert and Soehngen stated that the induced temperature and velocity fields had opposite influences on the Nusselt numbers of downstream tubes. For tubes directly over each other the temperature

difference between the tubes and air, in the immediate vicinity of the tubes, is less due to the warm wake from the lower tubes. This causes a reduction of the heat transfer from the upper tubes and therefore the Nusselt number, when based on the temperature difference between the tubes and the ambient air, is lower for the upper tubes than for the lowest tube. When the tubes were in the staggered arrangement, the middle tube has a higher Nusselt number. It is not completely in the wake of the first tube and the induced velocity of the wake increases the heat-transfer rate. The highest tube of the staggered arrangement is not completely in the wake of the second tube so that there is a strong velocity effect in increasing the Nusselt number, but at the same time, the warm air wake from the lowest tube tends to decrease the Nusselt number by decreasing the heat-transfer rate. The net result of these two effects on the highest tube is that the resulting Nusselt number is lower than that of the middle tube in the staggered array, but higher than the Nusselt number of the third tube in an unstaggered array.

Single cylinders and wires have been studied intensively. McAdams [2], in 1942, considering the results of many studies, presented a dimensionless correlation of Nusselt number versus Rayleigh number for single horizontal cylinders. The Rayleigh number range of the data was from  $10^9$  to  $10^{-4}$ .

In 1954 Collis and Williams [3] studied the effect of conduction in the axial direction on heat transfer from horizontal wires in natural convection. For wires in air they found that the axial conduction effect becomes negligible for a length diameter ratio greater than 20 000. Collis and Williams also extended the data for horizontal wires to lower Rayleigh numbers ( $10^{-3}$ – $10^{-9}$ ). For similar values of Rayleigh number, the work of Collis and Williams agrees with the suggested correlation of McAdams.

The temperature and velocity distributions within the plume above a horizontal line source (in experiments, a heated wire) has been the

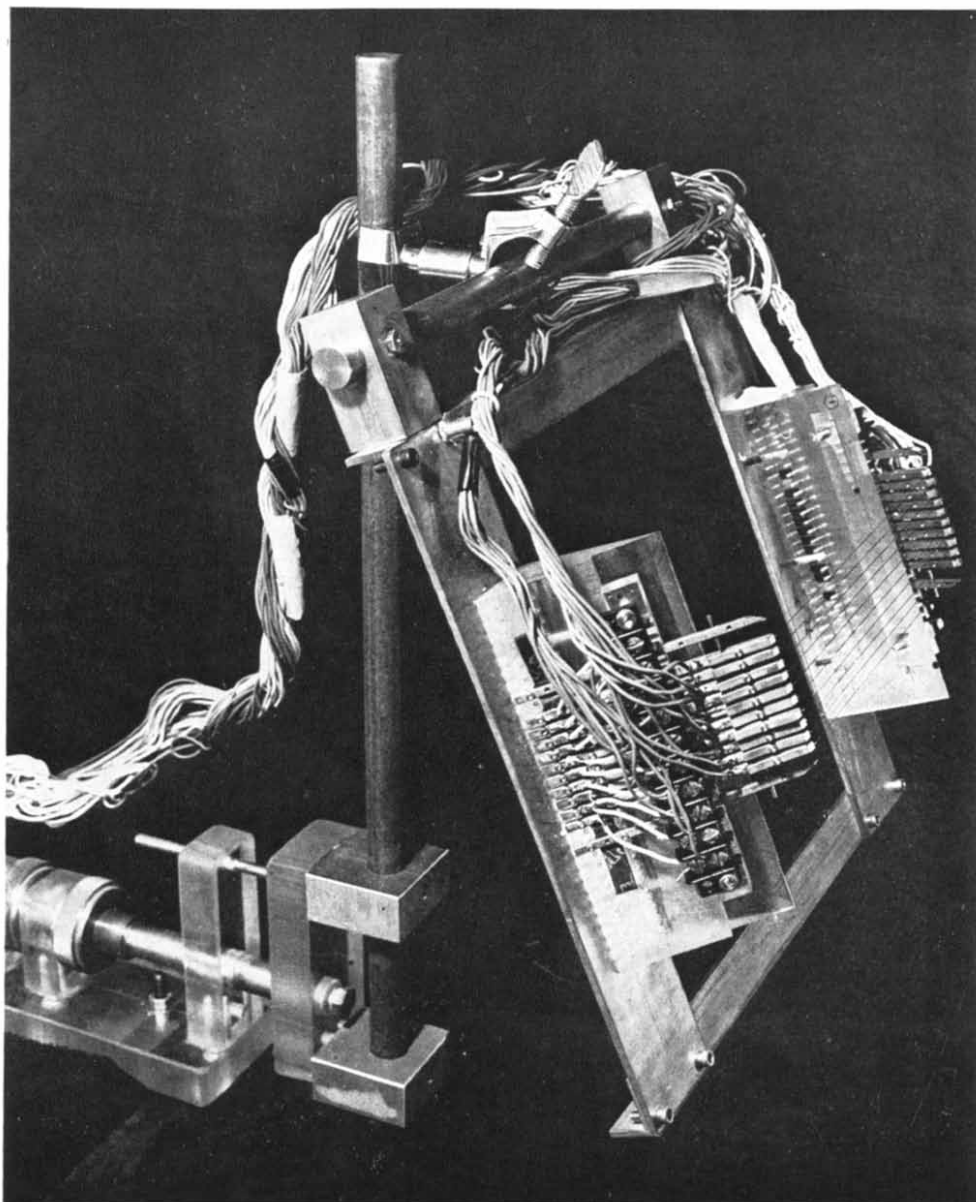


FIG. 1. Wire holder.

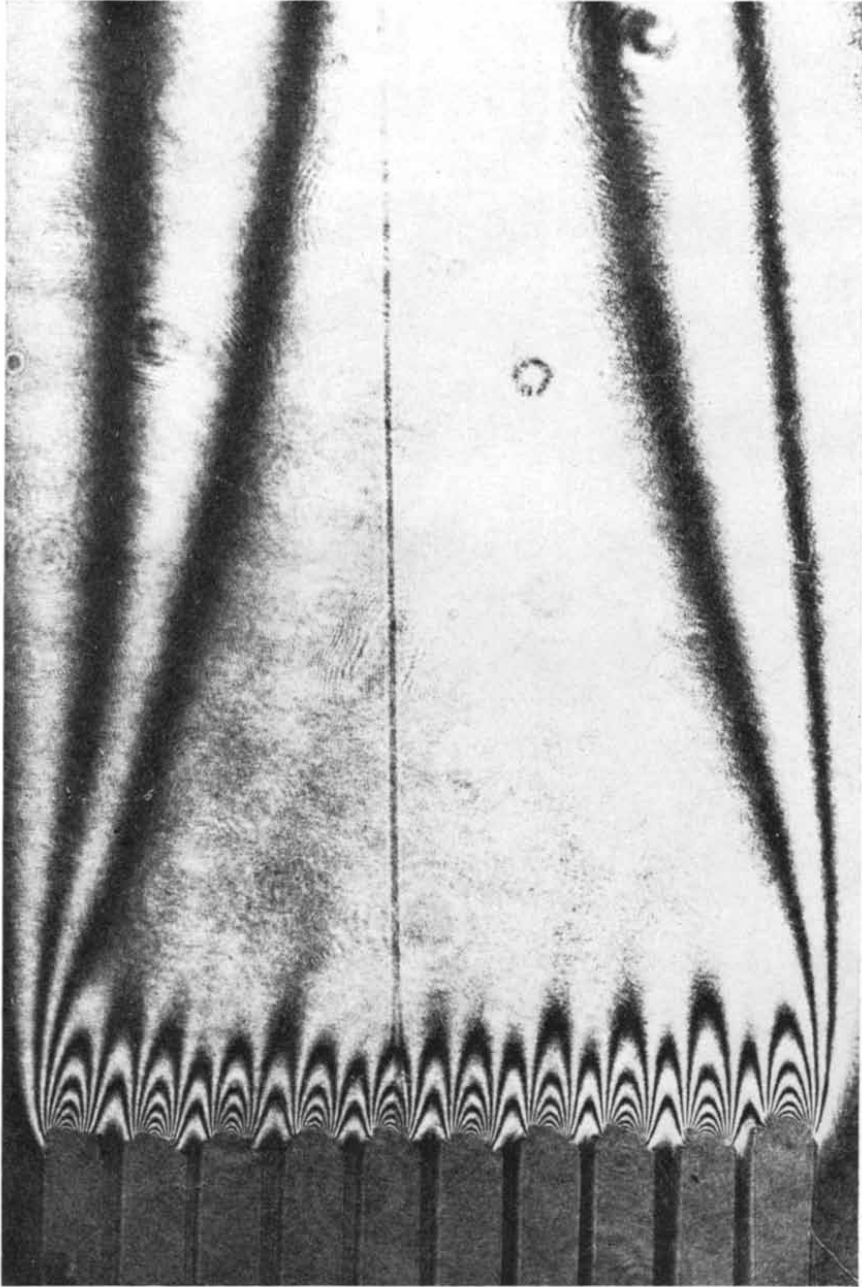


FIG. 3. Interferogram of the array angle  $90^\circ$ , 0.1875 in. spacing.

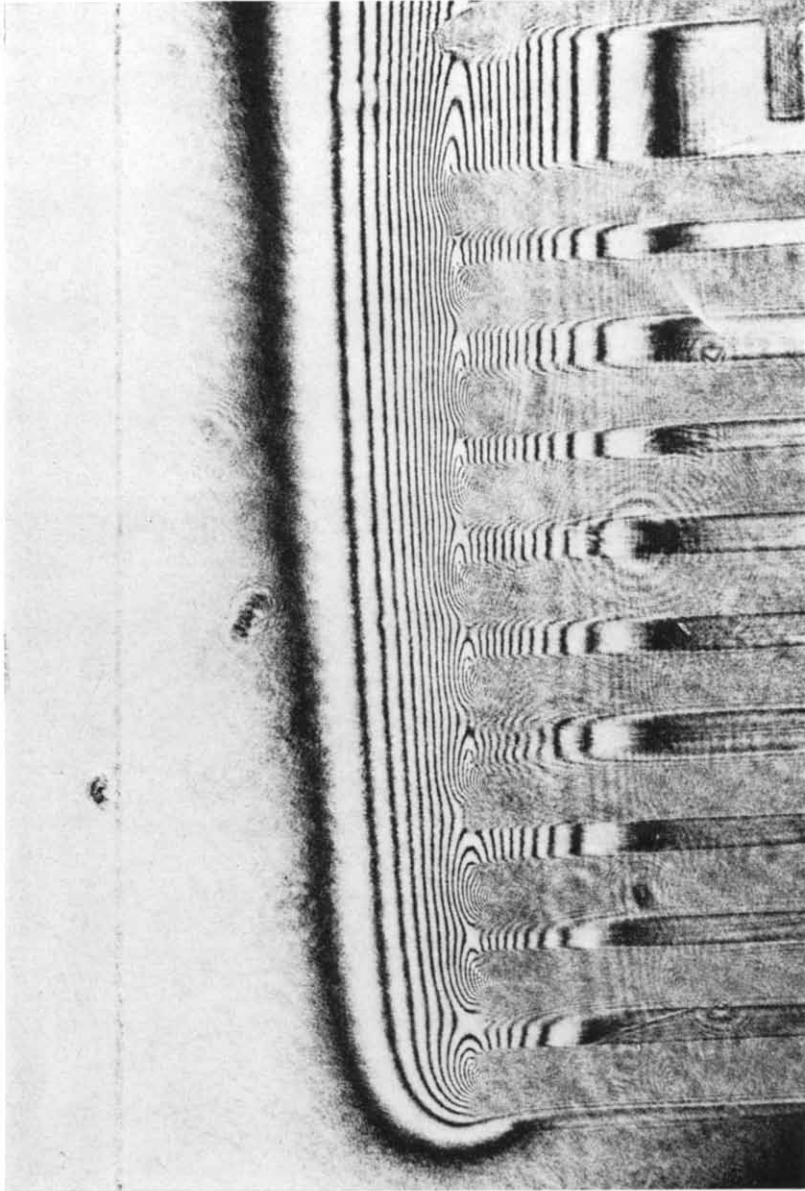


FIG. 5. Interferogram of the array angle  $0^\circ$ , 0.1875 in. spacing.

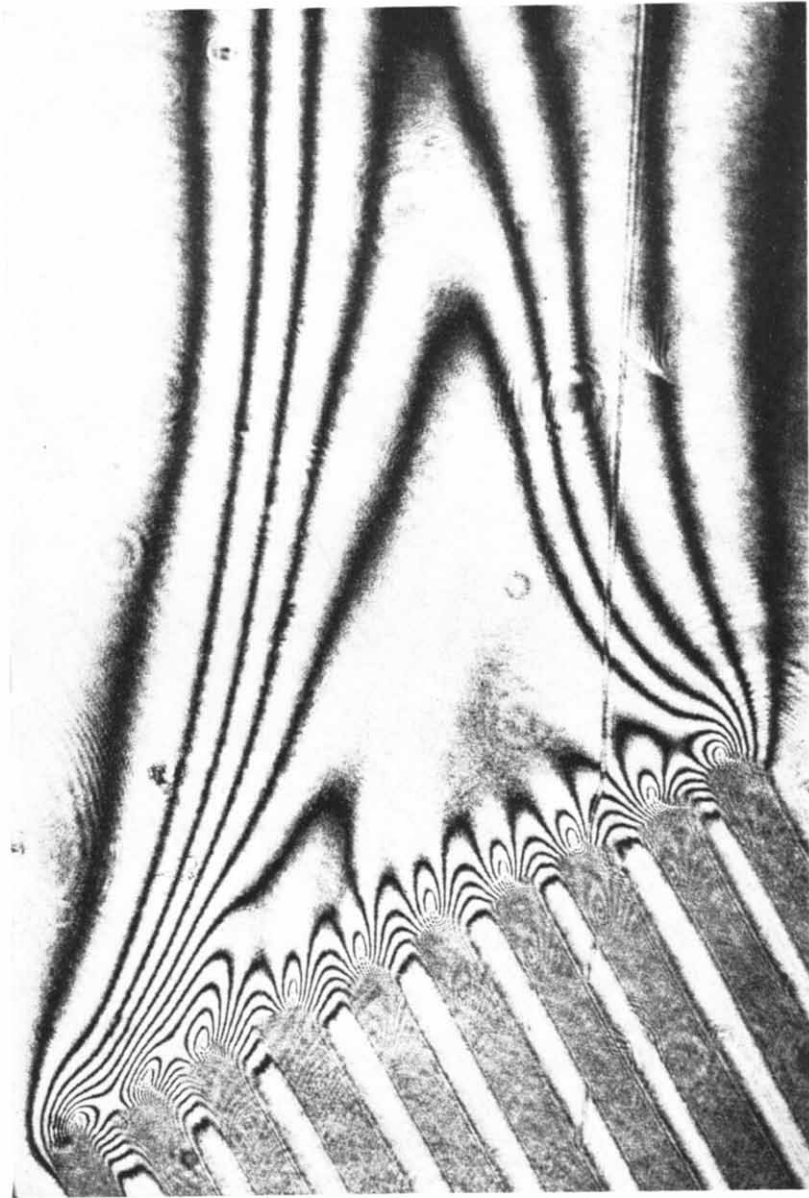


FIG. 10. Interferogram of the array angle  $60^\circ$ , 0.1875 in. spacing.

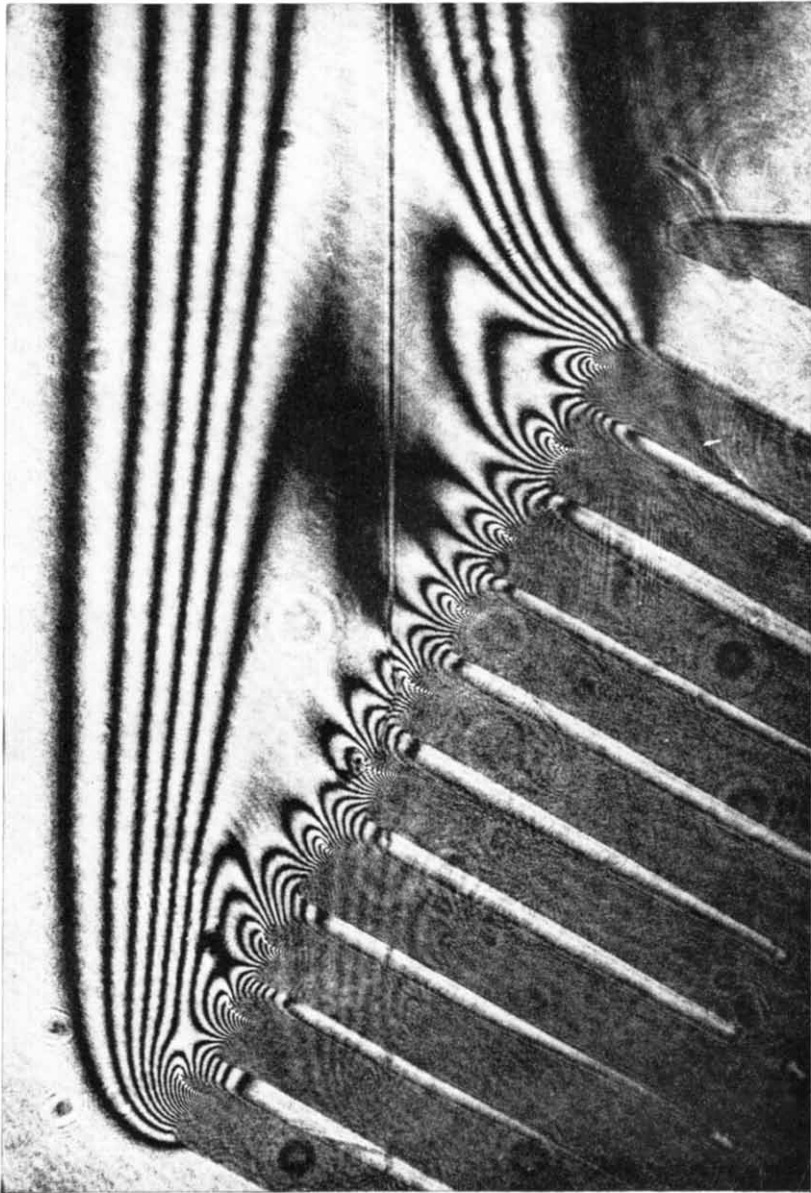


FIG. 11. Interferogram of the array angle  $30^\circ$ , 0.1875 in. spacing.

subject of many analytical studies. The problem was also studied experimentally in 1966 by Brodowicz and Kierkus [4]. The temperature and velocity distribution were measured. These measurements showed that cool air is induced into the plume from the sides and below the source. In 1967 Forstrom and Sparrow [5] also did some measurements of temperature above a wire source.

It is noted here that boundary layer theory for a plume above a horizontal line source gives the following results.

- (1) The centerline temperature of the plume decreases as the inverse of the three-fifths power of the distance above the source.
- (2) The centerline (i.e. maximum) velocity in the plume increases as the fifth power of the distance above the source.

The results for horizontal sources, discussed above, were used in our experimental investigation and interpretations of finite flat arrays of long, uniform flux, horizontal wires. The individual wire Grashof number for our experiments, based on the diameter, was  $1.75 \times 10^{-2}$ .

#### THE EXPERIMENTAL INVESTIGATION

The experimental program consisted of two parts. In the first part, temperature distributions were determined in the boundary region around the wire array, and in the plume above, with a Mach-Zehnder interferometer. The second study determined the heat-transfer characteristics of the individual wires by measuring the temperature of and heat flux from the wires. The Nusselt number was then calculated. Each individual wire in the array was used as a resistance thermometer, to determine its temperature.

Flat arrays of wires with different spacings were placed at different inclinations from the vertical. For the temperature distributions, twenty-four different combinations of wire spacing and array angle were used, to study the interaction of the individual wire plumes. Sixteen different combinations of spacing and orienta-

tion were used for the heat transfer part of the study.

#### EXPERIMENTAL APPARATUS

The wire holder assembly is shown in Fig. 1. Due to the physical limitations in the size of the wire holders the minimum wire spacing that could be used was 0.1875 in., or 37.5 wire diameters for the 0.005 in. dia. wire. Each of the ten wires within the array was mounted on a pair of 0.125 in. square brass rods, as shown in Fig. 2. Each brass support rod was attached to

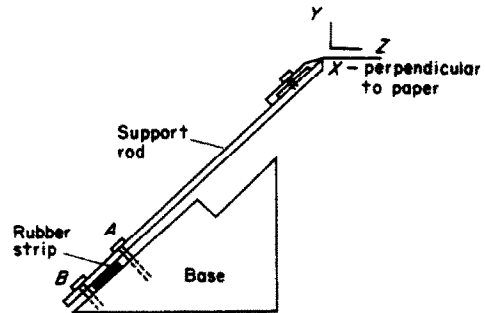


FIG. 2. Cross section of wire holder.

the base of the holder by two screws over a thin strip of gasket rubber. By the proper tightening of these screws the compression of the rubber strip acted as a spring for each wire support rod.

The 0.005 in. dia. wires were Nichrome with a nominal length of 7.25 in. This gave the wires a length to diameter ratio of 1450. Longer wires were preferred, to give a larger length to diameter ratio, but the width of the interferometer test section limited the maximum length.

At each end of the wire holder assembly a short 0.0625 in. dia. rod was placed through a brass support perpendicular to the wires. These served as guide posts for setting the wires parallel to the collimated light in the interferometer.

Two lead wires were attached to each support rod, one for the wire heating current and one for the voltage measurement. The voltage drop across each wire was measured. The current was determined by measuring the voltage over a 1  $\Omega$  Leeds and Northrup standard resistance,



in series with the heating wire. A digital voltmeter was used. The resistance of each wire could then be found. The resistivity-temperature dependence of the wire material was separately determined. The cold resistance of each wire was determined in place by a trickle current. From the measurements, the temperature and heat-transfer coefficient of each wire could be found.

The temperature distribution around the wire array was observed with a 5 in. Mach-Zehnder interferometer. A large box ( $5 \times 3 \times 4\frac{1}{2}$  ft) was constructed to cover the interferometer, in order to isolate the test section from stray air currents. However there was still some slight air currents as can be seen in the asymmetry of Fig. 8. The box was large enough so that no noticeable stratification occurred during a test. The infinite fringe method was used for the interferograms.

This interferometer was originally used with a mercury vapor light source with an interference filter passing light around a wavelength of 5460 Å. It was aligned using the method explained by Gebhart and Knowles [6].

The mercury source was replaced by a 7 mW Spectra Physics Stabilite Helium-Neon laser for this experiment. This had a wavelength of 6328 Å. The interferometer was first adjusted with the concentrated laser beam. This beam was used directly for the near and far cross hair adjustment, instead of a fixed cross hair. When the beams coincided at the two points there were fringes present. An expanding lens was added with a collimator to fill the five inch mirrors and beam splitters.

While collimating the input, an extra set of fringes appear after the first beam splitter. When the beam is collimated, these fringes disappear. This is a quick and very accurate way to find exact collimation.

Due to the Gaussian energy distribution from the laser, an  $f/6.7$  expanding lens was used for the laser while the collimating mirror was a 12 in.  $f/5$  which was stopped down to a 5 in.  $f/12$ . This permitted the use of just the more uniform center portion of the laser beam.

In order to obtain the highest contrast fringes with the filtered mercury vapor source, it was necessary to adjust the interferometer for the white light fringe by translating one of the interferometer mirrors. However, with the laser, the fringes did not improve in quality as the mirror was translated, due to the long coherence length of the laser light.

Using information from the International Critical Tables [7] for a laser wavelength of 6328 Å in air at 1 atm, an object length of 7.25 in., and an ambient temperature of 80°F, the number of degrees per fringe was calculated by the method of Polymeropoulos [8] as 6.67°F per fringe.

The temperature distributions were obtained from interferograms photographed with a Graflex x1 camera. Fringe location was determined with an optical comparator at a magnification of 10.

In the determination of temperature distributions by interferometry, the spacing between the wires and the array's angular orientation were varied so that there were twenty-four different combinations. The four angles were: 0° (vertical), 30°, 60° and 90°; the six spacings were: 0.1875, 0.3750, 0.5625, 0.750, 0.9375 and 1.125 in. These spacings correspond to 37.5, 75, 112.5, 187.5 and 225 wire diameters.

In determining individual wire heat-transfer results, sixteen different combinations of array angle and wire spacing were studied. The angles were: 0° (vertical), 30°, 60° and 90°; and the spacings were: 0.1875, 0.3750, 0.5626 and 0.750 in. Spacings of 0.9375 and 1.1250 in. were not used for the heat-transfer data because only two heated wires remained in the array at these wide spacings.

For the runs at other than the closest spacing, wires which were not heated were not removed from the holder. This procedure was followed because previous checks had shown that there were no noticeable changes between interferograms with the unheated wires removed from the wire holder, and with them remaining in place.

**EXPERIMENTAL RESULTS AND OBSERVATIONS**

**(A) Temperature distributions**

The coordinate system for the different geometric configurations is shown in Fig. 2. The origin of  $X$  is at the leading edge (lowest wire) of the array and of  $Y$  at the wire plane.  $Z$  is measured parallel to the wires. As the array was turned through the different angles the coordinate system remains fixed to the wire holder. The orientation angle is measured from the vertical position.

Twenty-four different interferograms were photographed, one for each angle-spacing combination. The four reproduced in this paper are those for the closest wire spacing used, 0.1875 in. (37.5 diameters) and for each of the four different angles:  $0^\circ$  (vertical),  $30^\circ$ ,  $60^\circ$  and  $90^\circ$ .

It should be emphasized here that spatial temperature distributions were measured by locating the center of the fringes. On the figures, such points were connected by straight lines. No interpolations were made to fractions of a fringe. Near the center of some of the plotted distributions horizontal lines occur which indicate regions where the temperature difference is less than one fringe ( $6.67^\circ\text{F}$ ). See, for example, Fig. 7.

The interferogram for the horizontal position ( $90^\circ$ ) is shown in Fig. 3. Ten distinct plumes are seen beginning at the plane of the wires. The interferograms were converted to temperature distributions (with  $X$ ) at different values of  $Y$  above the wires. Figure 4 shows that at  $Y = 0.013$  in. (2.6 diameters) the temperature distribution is jagged with peaks of high temperature above each wire. Due, apparently, to the flow induced by the array, there are higher maximum temperature peaks at the sides of the array than in the middle.

As  $Y$  is increased, there is more interaction between the plumes. The maximum temperatures decrease and the minimum temperatures increase. Eventually, at  $Y = 0.285$  in. (57 diameters), individual plumes are no longer distinguishable. Very much further above the plane of the wires the temperature distribution will no

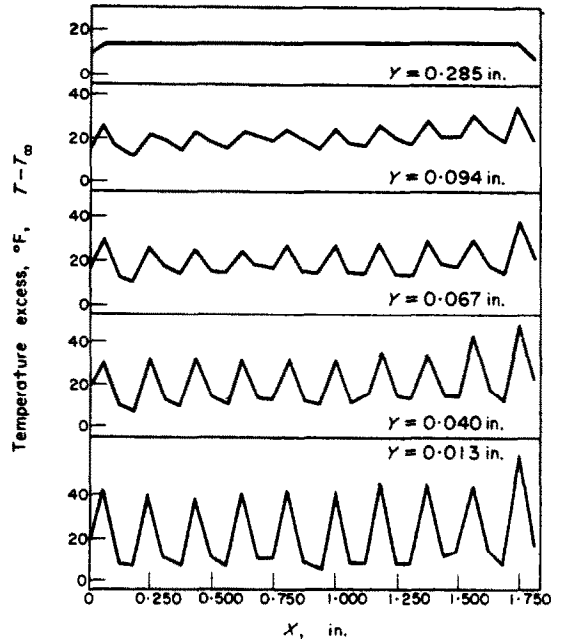


FIG. 4. Temperature distributions angle  $90^\circ$ , 0.1875 in. spacing.

doubt resemble a plume arising from a single source, eventually from a point source.

When the wire spacing was doubled, to 0.375 in., there was less interaction between the plumes near the wire plane, as might be expected. However, it was observed that there were again increasing interactions with increasing  $Y$ .

At 0.5625 in. spacing the higher wire temperature on either edge of the array was no longer observed, since apparently the plumes were completely separate near the plane of the wires. Below  $Y = 0.229$  in. (45.8 diameters) there is almost no interaction and in this region the maximum temperature was observed to decrease with  $Y^{-1/2}$ , as boundary layer theory indicates for a plume from a single line source. Again, far above the array the distributions began to look like a plume from a single source.

The temperature distributions for the spacings of 0.375, 0.750, 0.9375 and 1.125 in. all show that, with increasing  $Y$ , there is a smoother temperature distribution resulting from the widening of the temperature peaks.

The fringes very close to the wires were usually not differentiable, due to diffraction and Schlieren effects. Therefore, the temperature distributions for the 0° (vertical), 30° and 60° arrays were determined at a location midway between each wire in the Y direction, i.e. normal to the plane of the wires. With larger spacings, the distributions were still taken midway between all adjacent wires (heated and unheated). In the figures the distributions taken above heated wires are marked with an asterisk.

The interferogram for the vertical position is shown in Fig. 5. The support rods are on the right side of the photograph. A plume effect may be seen around each wire but, as seen in the interferogram, they quickly merge with the growing boundary region surrounding the array. The temperature distributions for the closest spacing (0.1875 in.) appears in Fig. 6. As X

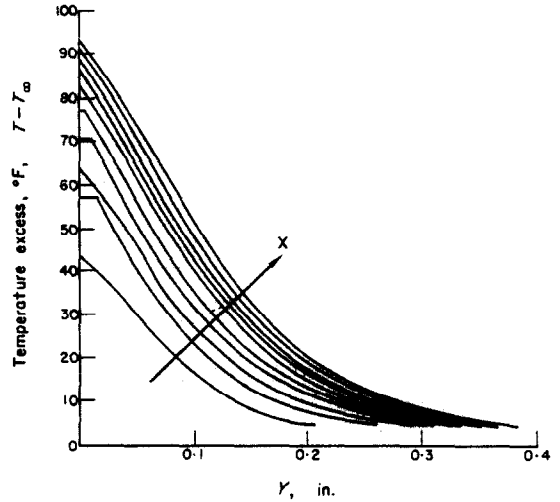


FIG. 7. Superimposed temperature distributions angle 0°, 0.1875 in. spacing.

more clearly seen in Fig. 7, where the distributions have been superimposed.

When the spacing was increased to 0.375 in. for the vertical array, as shown in Fig. 8, the maximum temperature above the second wire, which was unheated, was less than the maximum temperature above the first wire, which was

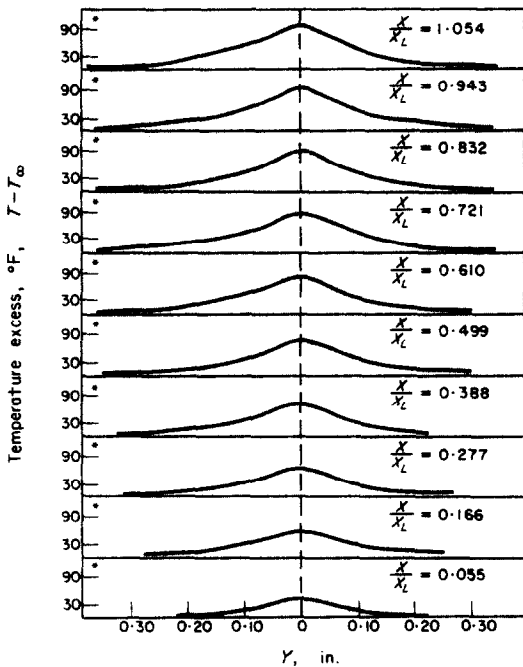


FIG. 6. Temperature distributions angle 0°, 0.1875 in. spacing.

increases the maximum temperature in each distribution also increases and the width of the boundary region slightly increases. This is

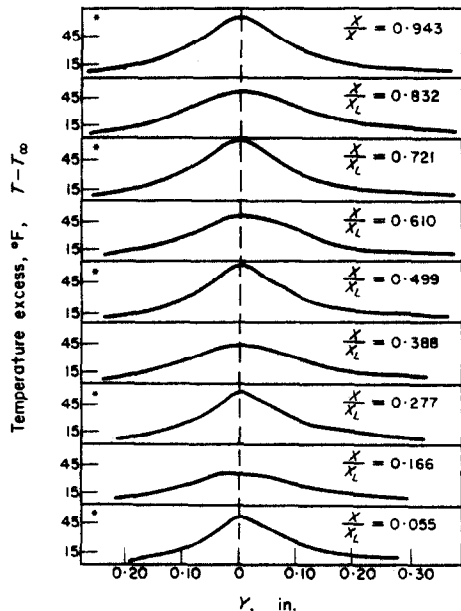


FIG. 8. Temperature distributions angle 0°, 0.375 in. spacing.

heated. Each distribution above a heated wire had a maximum temperature that was greater than the maximum temperature in the distribution above the previous heated wire; and also each distribution above an unheated wire had a maximum temperature that was again greater than the one in the distribution over the previous unheated wire.

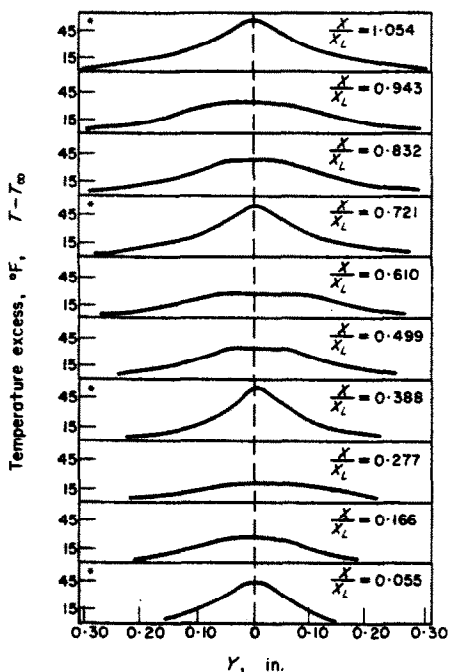


FIG. 9. Temperature distributions angle  $0^\circ$ , 0.5625 in. spacing.

This is again seen in Fig. 9 with the array at a spacing of 0.5625 in. There is now a second unheated wire which has a distribution with a lower maximum temperature than the maximum temperature in the distribution over the unheated wire directly below it. As  $X$  increases up the array, there is a cycle of this pattern, each cycle at a higher temperature level.

As the spacing was further increased, the distributions over each heated wire became more similar to the one above the first heated wire. The rest of the spacings studied had this same pattern, with the number of distinct cycles equal to the number of wires heated.

The interferograms for the array at  $60^\circ$  and  $30^\circ$ , at the 0.1875 in. spacing, are shown in Figs. 10 and 11. The corresponding temperatures are plotted in Figs. 12 and 13. Both of these

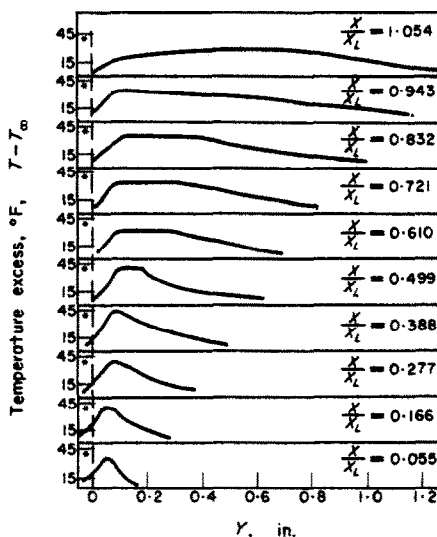


FIG. 12. Temperature distribution angle  $60^\circ$ , 0.1875 in. spacing.

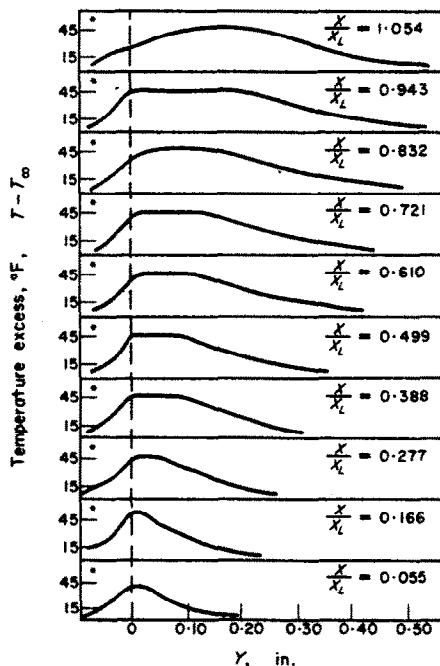


FIG. 13. Temperature distribution angle  $30^\circ$ , 0.1875 in. spacing.

interferograms show a strong side effect as the plume tries to climb up the array, as would happen with a flat plate at this angle. However, above the wires at both edges of the array the plume has broken away from the array, parallel to the direction of gravity. Far above the array neither of the two plumes is symmetrical with the center of the wireholder, as were the plumes for the vertical and horizontal orientations.

Above the first wire in each the  $60^\circ$  and  $30^\circ$  orientations the basic plume distribution is skewed. This is due to the distribution having been taken normal to the plane of the array. The distribution for the largest value of  $X$  is very different from the earlier distributions. The isotherms are breaking away from the top of the array. This effect is also seen in the interferograms (Figs. 10 and 11). As the spacing of the wires in the array at  $30^\circ$  and  $60^\circ$  is increased, the cycling effect found in the temperature distribution for the vertical orientation is also observed.

In interpreting the behavior of the arrays it was hoped to compare the merged downstream distributions to those of a plume above a heated wire, and the distributions in the boundary region of the array to that arising over a uniform flux flat plate at different angles. The distributions with the arrays at  $30^\circ$ ,  $60^\circ$  and  $90^\circ$  (horizontal) did not compare with the distributions of a flat plate at these angles because in the array the air flows between the wires. The boundary region thickness for the vertical orientation resembles that over a vertical flat plate but is relatively much thicker, even though an "array" Grashof number may be calculated as being the order of  $5 \times 10^4$ . It is likely that the boundary region of a much longer vertical array would approach more closely the behavior of a uniform surface flux flat plate. It was not possible to compare the distribution of the array's combined plume (relatively near the plane of the wires) to the plume arising from a single source, due to the distributed sources in the array. However, at very large distances above the wire holder, the effect of the distributed

sources should be so merged that the distribution would be similar to that far above a single source.

### (B) Heat transfer

While the interferograms gave the temperature distribution in the air around the array, the resistance thermometer method gave the temperature, the heat flux and, therefore, the heat transfer coefficient of each individual wire. The heat transfer coefficient used here is calculated on the basis of the difference in temperature between the wires and the distant ambient air ( $T_\infty$ ), and not from the wires to the air in the immediate vicinity of the wires, the latter being ill-defined.

Each wire in a given array was dissipating essentially the same amount of heat. The average heat transfer rate to the ambient air was 4.669 Btu/h per wire. The radiation losses were calculated for the maximum experimental temperature excess of  $170^\circ\text{F}$ . The calculation was based on the assumption that the total surroundings for each wire were at  $T_\infty$ . The emissivity of the nichrome wire was taken to be 0.1. The radiation loss was found to be less than 1 per cent of the total heat transfer and, therefore, radiation was ignored in the calculations.

For the four angles and the four spacings considered, it was found that the vertical array at the closest spacing had the highest average wire temperature, and, therefore, the smallest Nusselt number. Figure 14 shows the wire temperature distribution (wire temperatures normalized with the temperature excess of the first heated wire [ $T_{w0} - T_\infty$ ], and the  $X$  distance normalized with the width of the array,  $X_L$ ).

Results are shown for the vertical position ( $0^\circ$ ) for each of the four spacings studied. For the closest spacing, 0.1875 in., the wire temperature increased up the array. At the next wider spacing, 0.375 in., the temperature of the wires decreased up the vertical array, resulting in an average wire temperature that was lower than the average for the 0.1875 in. spacing array. The average temperature is taken as the arithmetic average of the individual heated wire

temperatures for any spacing. At the third spacing, 0.5625 in., the wire temperatures were still decreasing with increasing  $X$ , and the average array temperature reached a minimum. At the farthest spacing, 0.750 in., the wire temperatures still decreased with increasing  $X$ , but the average wire temperature was greater than for the previous spacing.

The wire temperatures and heat transfer coefficients for the horizontal ( $90^\circ$ ) and  $60^\circ$  arrays were similar to each other. In both orientations the wire temperatures were cooler in the center than at the edges of the array.

Figure 14 also shows that the wire temperatures of the array at  $60^\circ$  were consistently lower over a larger number of wires than for the horizontal orientation. It is also noted that the cooler portion of the array is not as symmetrical for  $60^\circ$  as for the horizontal position.

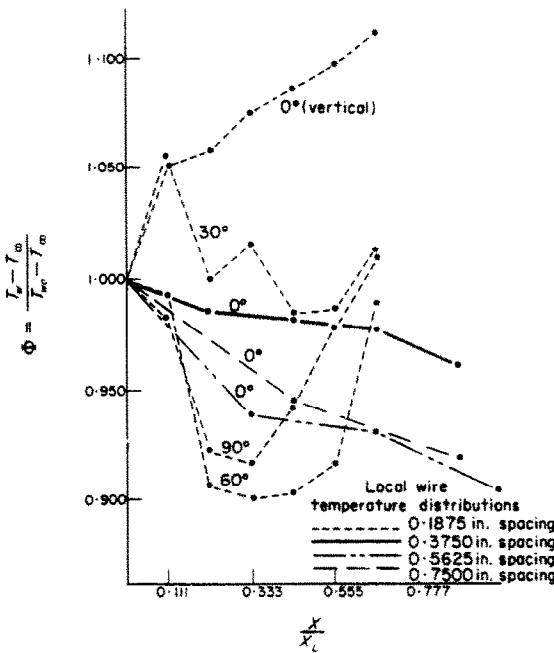


FIG. 14. Local wire temperature distributions.

With increasing spacing, for both  $90^\circ$  and  $60^\circ$ , the wires remained cooler near the center of the array. However, the average array temperature decreased at the second spacing and thereafter began to increase.

The three angular orientations,  $0^\circ$ ,  $60^\circ$  and  $90^\circ$ , showed definite patterns. However, the array at  $30^\circ$  had alternating wire temperatures. The second wire at this angle, as seen in Fig. 14, had a higher temperature than the first wire, the third wire's temperature was lower than the second, etc. In spite of this rise and fall in the temperature of alternating wires, the overall (average) effect is clearly a temperature decrease with increasing  $X$ . For larger spacings at this angle the alternations continued in the direction of decreasing temperature with the average wire temperature reaching a minimum at the second spacing. After that spacing the average wire temperature increased.

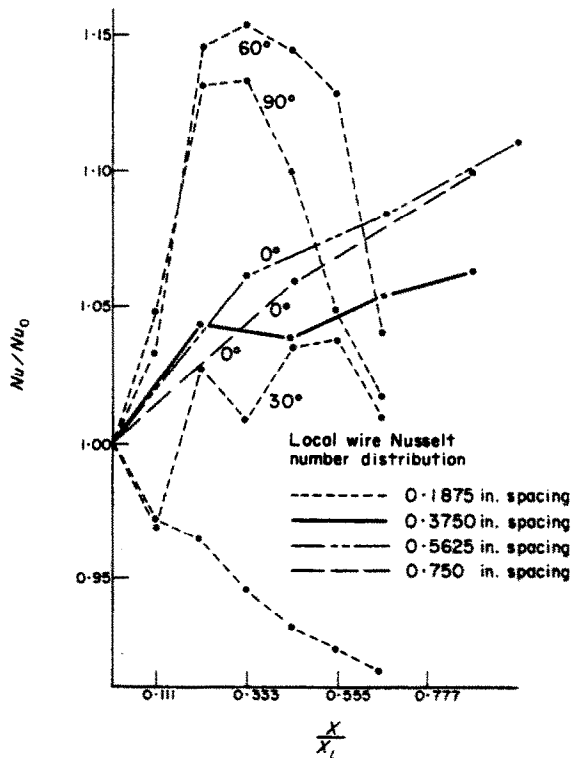


FIG. 15. Local wire Nusselt number distribution.

Figure 15 shows how the local Nusselt numbers, corresponding to the wire temperatures in Fig. 14, changed with  $X$ . The Nusselt number is normalized with the Nusselt number of the first heated wire,  $Nu_0$ . Since the heat flux is

constant, the heat-transfer coefficient varies inversely with the temperature excess, thus Figs. 14 and 15 are the inverse of each other.

The results of the heat-transfer data are summarized for the different angles and spacings in Fig. 16. This figure shows the average array Nusselt number as a function of spacing, expressed in wire diameters. The Nusselt numbers in this figure are the inverse of the average array wire temperatures, for the same reason that Figs. 14 and 15 are the inverse of each other. For all angular orientations, as the spacing increases, the Nusselt number increases to a maximum and then begins to decrease.

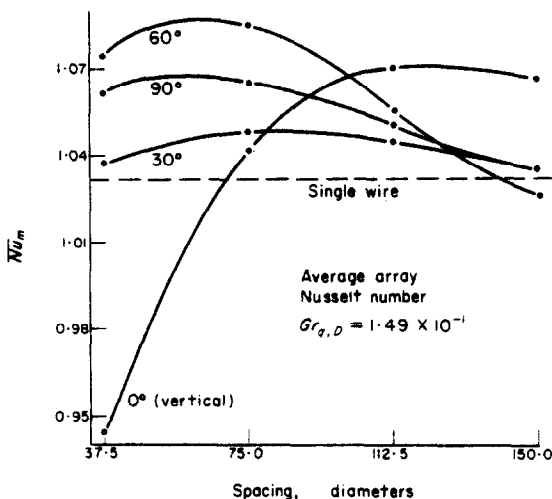


FIG. 16. Average array Nusselt number.

While further spacings were not investigated, it seems reasonable that at very large spacings the average Nusselt number and wire temperature will asymptotically approach the behavior of a single wire.

#### ERRORS AND ACCURACY

An error analysis of the measurements indicate that the temperature determinations have an accuracy of  $\pm 0.30$  per cent, and that the heat-transfer coefficients have an accuracy of  $\pm 0.75$  per cent.

It was found that the Nusselt number results (in Fig. 16) have an average standard deviation

of 1.06 per cent of the plotted mean values. While this is a large value, it does not shift the curves in Fig. 16 enough to vitiate any of the trends found.

As a further check of these results, the Nusselt number of a single wire was compared to the value predicted by the dimensionless correlation of McAdams [6]. The value found in this experiment was higher. However, the values considered by McAdams were based on experiments with very long wires. As mentioned in the introduction, Collis and Williams [3] reported that, in order to have a true infinite cylinder, a length to diameter ratio of 20 000 is necessary. In the present experiment the length to diameter ratio was 1450. By dividing our experimental Nusselt number by the factor of 1.3, suggested by Collis and Williams for horizontal wires for the ratio of 1450, the values obtained in this experiment, 1.032, is reduced to 0.793, for an infinite cylinder. This corrected Nusselt number is within 2 per cent of the value 0.785 obtained experimentally by Rice for the same Grashof number and used by McAdams in the correlation. The McAdams correlation curve is about 8 per cent lower than Rice's data and 10 per cent lower than the corrected Nusselt number determined in this experiment.

#### CONCLUSION AND DISCUSSION

The temperature distributions determined from interferograms indicated that the plumes interacted. Also, the spacings were too large, even at the closest spacing (37.5 diameters) for the induced flow field to approach the characteristics of that from an impervious flat surface.

It should be noted that this study refers to a finite array. The interferograms show that the isotherms in the boundary region break away from the downstream edge of the array for inclined orientations. Further investigations are necessary to learn if the isotherms would continue to break away from the upper edge of a longer array (more heated wires) or would remain attached as they do along the surface of a heated flat plate.

The temperature distributions around the

array of wires were distinctly affected by the variation of both spacing and array orientation angle. However, at some distance above the array the individual plumes were no longer distinguishable. In all cases they combine to form one large plume. This plume would eventually be similar to a plume arising from a single source.

At the closest spacing investigated for the vertical orientation (37.5 diameter) the wire temperatures increased up the array. Even though the temperature in the rising plume decreases by diffusion before reaching the second heated wire, the temperature of the air within the plume was still high enough to increase the wire temperature.

However, at the next spacing (75 diameters) the wire temperatures decrease with increasing  $X$ . This indicates that the temperature of the air in the plume has been reduced to a low enough value so that the dominant effect (which actually reduces the wire temperatures) is the increased air velocity (over simple stagnant surroundings) within the plume.

At the third spacing (112.5 diameters) the wire temperatures also decrease with increasing  $X$ . Over the distance the plume has travelled from the first wire to the second heated wire, the air temperature has been further reduced, by diffusion, at this third spacing, so that the further increased velocity results in a still lower wire temperature at the third spacing than for the second spacing.

For the widest spacing investigated with the vertical array (150 diameters), not only the plume's temperature is being diminished by diffusion but also, apparently, the air velocity, so that the latter wire temperatures, while still decreasing with increasing  $X$ , are higher than those at the previous spacing. One supposes that at very large spacings, both the plume's temperature and velocity may decrease enough so that the temperature of each later wire in the array will not be substantially influenced by the preceding wires.

While it was possible to explain the increasing

and decreasing wire temperatures of the vertical array with the theory of plume behavior above a line source, no simple explanation is available to explain the observations with the 30°, 60° and 90° (horizontal) orientations of the arrays. Measurements of the induced velocities must be made around the wires in the array to fully understand the reasons for:

- (1) The wire temperatures at the center of the array at 60° and 90° being cooler than at the edges.
- (2) The wire temperatures for the 60° orientation being cooler over a larger number of wires than for the 90° position.
- (3) The oscillation of wire temperatures along the array at 30°.

In conclusion, there is an optimum spacing at each array angle for a maximum Nusselt number to result. The highest average Nusselt number for the 16 different angle-spacings combinations occurred at a spacing of 75 diameters for the array at 60°. This is in partial agreement with the results of Eckert and Soehngen which suggested that a staggered array would give the maximum heat transfer.

#### ACKNOWLEDGEMENTS

The authors wish to acknowledge support for this research under National Science Foundation Grant GK1963 and support from the same grant for the first author as a research assistant.

#### REFERENCES

1. E. R. G. ECKERT and E. SOEHNGEN, Studies on heat transfer in laminar free convection with the Zehnder-Mach Interferometer, Tech. Rept. No. 5747, U.S.A.F. Air Material Command, Dayton, Ohio (1948).
2. W. H. MCADAMS, *Heat Transmission*, 3rd Edn, p. 176. McGraw-Hill, New York (1954).
3. D. COLLIS and M. WILLIAMS, Free convection of heat from fine wires, Australian Aeronautical Research Laboratories, Aerodynamic Note 190 (1954).
4. K. BRODOWICZ and W. T. KIERKUS, Experimental investigation of laminar free convection flow in air above horizontal wire with constant flux, *Int. J. Heat Mass Transfer* 9, 81-94 (1966).
5. R. J. FORSTROM and E. M. SPARROW, Experiments on the buoyant plume above a heated horizontal wire, *Int. J. Heat Mass Transfer* 10, 321-330 (1967).



6. B. GEBHART and C. P. KNOWLES, Design and adjustment of a 20 cm Mach-Zehnder interferometer, *Rev. Scient. Instrum.* 37, 12-15 (1966).
7. *International Critical Tables*, Vol. 7. McGraw-Hill, New York (1930).
8. C. E. POLYMERPOULOS, A study of the stability of free convection over a uniform flux plate in nitrogen, Ph.D. Thesis. Cornell University (1966).

**Résumé**—Les interactions entre les écoulements décollés de convection naturelle provoqués par des surfaces individuelles dans un arrangement à faible écartement sont étudiées pour différentes dispositions d'espacement et d'orientation. Les effets sur le transport de chaleur et sur l'écoulement provoqué et le champ de température sont déterminés. Les causes des différents effets sont déduits des interférogrammes du champ de température voisin et du panache qui s'élève. Certaines relations entre les effets sont apparentes et sont explicables en termes physiques directs, bien qu'aucune théorie ne soit donnée. Il est clair à partir de ces résultats que les effets d'interaction peuvent être optimisés de façon profitable pour des buts particuliers.

**Zusammenfassung**—Es werden die Wechselwirkungen der von verschiedenen Oberflächen induzierten natürlichen Konvektionsströme studiert. Diese Oberflächen sind in geringem Abstand zueinander angeordnet, der Abstand und die gegenseitige Orientierung wird verändert. Die Auswirkungen auf den Wärmeübergang, den induzierten Strom und das Temperaturfeld werden bestimmt. Die Ursachen verschiedener Effekte werden aus Interferogrammen des Nahtemperaturfeldes und der aufsteigenden Strömungsfigur gefolgert. Bestimmte Reaktionen zwischen den Effekten sind offensichtlich und durch direkte physikalische Beziehungen erklärbar, obwohl keine Analyse durchgeführt wurde. Von diesen Ergebnissen her ist es einleuchtend, das Wechselwirkungseffekte für bestimmte Zwecke vorteilhaft optimiert werden können.

**Аннотация**—Исследовалось взаимодействие между отдельными потоками естественной конвекции, вызванными на отдельных поверхностях, расположенных близко друг от друга, для различных расстояний между поверхностями и их ориентаций. Определялось влияние этих факторов на перенос тепла, индуцированное течение и поле температур. Причины различных эффектов определялись по интерферограммам. Видна определенная взаимосвязь между эффектами, что можно объяснить физически, однако анализа не приводится. На основании полученных результатов можно сделать вывод, что для определенных целей эффекты взаимодействия можно выгодно оптимизировать.